The Effects of Ionizing Radiation on TaO_x-based Memristors

B. D. Tierney[1], H. P. Hjalmarson[1], M. L. McLain[1] and D. R. Hughart[1]
[1]Sandia National Laboratories, Albuquerque, NM

ABSTRACT:
The irradiation of tantalum oxide memristors is simulated. Tunneling transport through device interfaces is considered and transport characteristics are compared with recently published experimental data of memristor devices subjected to pulsed ionizing radiation.

Corresponding (and Presenting) Author:

Brian D. Tierney

Sandia National Laboratories

P.O. Box 5800, MS 1320, Albuquerque, NM, 87185-1320

Phone: 505-284-3029

Email: bdtiern@sandia.gov

Co-Authors:

Harold P. Hjalmarson	Sandia National Labs	Email: hpjalm@sandia.gov	Phone: 505-844-8888
Michael L. McLain	Sandia National Labs	Email: mlmclai@sandia.gov	Phone: 505-844-6825
David R. Hughart	Sandia National Labs	Email: dhughar@sandia.gov	Phone: 505-844-3153

Session Preference: Basic Mechanisms of Radiation Effects in Electronic Materials and Devices

Presentation Preference: Oral

FUNDING STATEMENT
This work was funded by Sandia's Laboratory Directed Research and Development program. Sandia National Laboratories is a multi-program laboratory managed and operated by Sandia Corporation, a wholly owned subsidiary of Lockheed Martin Corporation, for the U.S. Department of Energy's National Nuclear Security Administration under contract DE-AC04-94AL85000.

INTRODUCTION

As silicon-based memory technologies rapidly approach scaling limits, the semiconductor research community is actively pursuing novel device technologies to replace static random access memory (SRAM), dynamic RAM (DRAM), and flash memories. In fact, several candidate technologies have emerged in recent years as possible replacements for the aforementioned technologies. One particularly promising technology that has been identified as such by the International Technology Roadmap for Semiconductors (ITRS) is resistive RAM, also known as redox, memristive memory, or ReRAM. ReRAM structures are comprised of an array of two terminal metal-insulator-metal *memristors* that are characterized by a low resistance on-state and a high resistance off-state. Such states depend on both the electrical bias and bias history. Examples of commonly used insulators being researched for ReRAM memory devices are the transition metal oxides (TMOs) such as tantalum oxide (TaO_x), titanium dioxide (TiO_2), and hafnium oxide (HfO_x). [We note that the subscript x in TaO_x denotes that the material is substoichiometric tantalum pentoxide (Ta_2O_5)].

Tantalum oxide memristors are particularly attractive in this regard because of their excellent scalability, high endurance, high switching speed, and low voltage operating regime [1-3]. The switching mechanism in TaO_x memristors involves redox reactions and the migration of O^{2-} anions and oxygen vacancies. These processes lead to the formation of a Ta-rich conducting filament of a certain radius [4],[5]. As a result, these and other oxide-based memristors exhibit a characteristic *I-V* hysteresis whereby one of the two paths of the hysteresis curve in the low-bias regime represents a high resistance off-state, and the other a low resistance on-state.

While previous modeling studies have discussed memristor behavior as due to the diffusion of oxygen vacancies, a sound model for the electronic current and vacancy diffusion mechanisms at the metal-insulator junction has yet to explain experimental observations. Thus, in this work we investigate the role that tunneling plays in the transport properties of tantalum-oxide memristors. Additionally, given the potential use of TaO_x memristors in radiation-hardened electronics, it is imperative to be able to adequately model the radiation susceptibility of these devices. Hence, initial results are presented of our theoretical study of pulsed ionizing radiation on a TaO_x-based memristive technology. These studies are being conducted in conjunction with a concurrent experimental study on memristor radiation susceptibility [6].

SIMULATION MODEL

For oxide and semiconductor devices, the Sandia Radiation Effects in Oxides and Semiconductors (REOS) code iteratively solves the reactive transport equations for a set of carrier species for device structures defined by a spatially non-uniform mesh. The governing kinetic equation is

$$\frac{\partial c_i}{\partial t} = \nabla \cdot \boldsymbol{J}_{si} + \sum_j \nu_{ij} R_j + G_i \ , \tag{1}$$

in which $c_i \equiv c_i(\boldsymbol{r},t)$ denotes the species concentration as a function of position $\boldsymbol{r}$ and time t, $\boldsymbol{J}_{si}$ is the species current density, R_j is the reaction rate for defect reaction j, and G_i is the species generation rate due to a non-defect incident that could occur, for example, due to an ionizing radiation event. The stoichiometric coefficient ν_{ij} describes the contribution of reaction j to species i. In a drift-diffusion approximation, the key current contribution arises from electrons: $\boldsymbol{J}_{si} = n\bar{\mu}_n \nabla\phi - T_n \bar{\mu}_n \nabla n$, in which n is the electron density, φ is the electric potential, $\bar{\mu}_n$ is the electron mobility and T_n is the electron temperature. This current can also be written as a gradient of the electrochemical potential $\Phi_n = -\varphi + \mu_n$, in which μ_n is the chemical potential (quasi Fermi energy) for electrons. The electrochemical potential, generalized to all species involved in these devices, is a central quantity in our calculations. The

electrostatic potential is obtained by solving the Poisson equation $\nabla^2\phi = -\rho/\varepsilon$, in which $\rho = \sum_i \nu_i c_i$ is the total charge density (ν_i is the charge of the species concentration c_i) and ε is the dielectric constant. In these calculations, the chemical potential μ_i is assumed to take the form $\mu_i = \mu_{0i} + kT \log\left(Q_i / c_i V\right)$, where μ_{0i} is a material dependent constant, Q_i is the species partition function, and V is the volume of the region such that the chemical potential may be considered a constant value, μ_i. REOS also calculates displacement current in the determination of transient quantities, and Joule heating is accounted for by solving the Fourier heat equation. Most importantly, REOS accounts for radiation effects, interface tunneling, and defect chemistry.

In particular, the defect reaction in oxide-based memristors between neutral and singly charged oxygen vacancies, D^0 and D^+ respectively, is essential to our model: $D^+ + n \leftrightarrow D^0$. The forward and reverse reaction rates from this defect reaction are obtained from the reaction cross section and thermal velocity. The effects of doubly charged oxygen vacancies are included in some calculations.

Tunneling through the metal-oxide interfaces is included in the model via a modification of the local generation and recombination rates by calculating the electron tunneling current using the WKB approximation [7]. Band-to-defect tunneling is also included by the inclusion of defect reaction equations between cells joined by tunneling. Finally, Poole-Frenkel tunneling from defect states is also included in some calculations.

SIMULATION DETAILS & RESULTS

The calculations to be described are motivated by previous work on the effects of ionizing radiation on TaO_x devices [6]. Data for three devices from this previous study are shown in Fig. 1. This figure shows that the radiation pulses cause a photocurrent that is larger than the dark current for each of three different devices. In the following discussion we first focus on this photocurrent.

The observed photocurrent in Fig. 1 is very large given the small active volume of these devices. The photocurrent can be estimated by using the relation $I = qGV$ in which G is the dose rate and V is the active volume of the device. The active TaO_x region of each device has a 10 nm thickness and sides of length 250 nm giving an approximate volume $V = (1/16)\times10^{-14}$ cm^{-3}. For the given dose rate $G = 5\times10^{21}$ s^{-1}cm^{-3}, the current $I \approx 0.3\times10^{-12}$ A. This current is smaller than the measured current $I_e \approx 10^{-5}$ A by a factor of 10^7.

The initial calculations produced a similar result. These calculations were applied to a simple defect free structure with an active region thickness of 30 nm (this discrepancy with the sample oxide thickness will be corrected in future calculations). The band offsets are chosen to be small (0.35 eV) to reproduce the dark current. These results, also shown in Fig. 1, are comparable with the three sets of data. However, the dose rate used in the calculation has been increased by the 10^7 factor in order to make these calculations comparable with the data.

To eliminate concerns about the REOS calculations, they were validated by comparing them with equivalent calculations performed by using the commercial device simulation software Silvaco Atlas. These comparisons were made on a silicon slab uniformly irradiated. The REOS and Silvaco calculations agree to within 2% (see Fig. 2).

These initial calculations also suggest that the first theoretical task should be to develop mechanisms that explain the dark current. For example, a simple band offset barrier would allow negligible dark current unless the band offset barriers are small enough to allow thermionic current to flow. However, such a current is inconsistent with the fact that these structures can be very non-conductive.

Oxygen vacancies are assumed to control the conductivity of these structures, but conclusive information about their role in transport during irradiation by ionizing radiation is not available. These

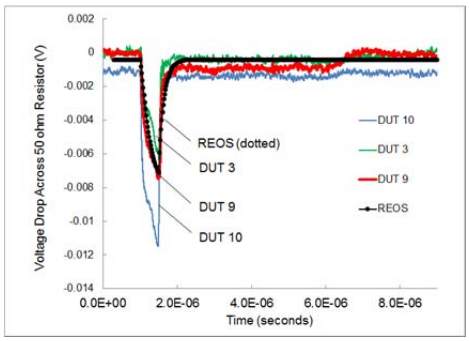

Figure 1: Simulated and experimental memristor transient response due to a 500ns ionizing radiation pulse with a 0.1 V bias voltage. The experimental curves are described in [6]. The REOS results use an enhancement factor as described in the text.

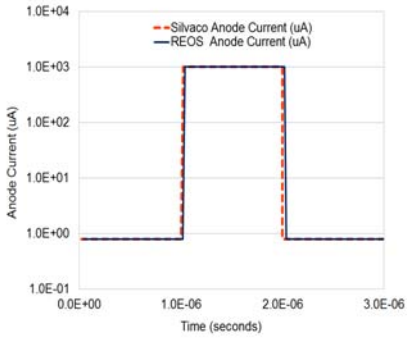

Figure 2: Comparison of REOS and Silvaco I-V characteristics of a $1x10^{14}$ cm^{-3} n-doped 50nm silicon slab (250nm x 250nm cross section) as a result of applying a 1us ionizing radiation pulse with a 0.1 V bias voltage.

defects are assumed to be present in high density, but their ionization energies are large (1 eV). Furthermore, the band offsets of the active regions with electrodes are not well known.

This absence of information led to an approach in which general mechanisms of transport are assumed. Thermionic emission is included in all calculations. For most calculations, free-electron to defect tunneling is included. In another series of calculations, free-electron tunneling to free-electron states in the oxide is included. This effect can be important if the vacancies have small ionization energies. Finally, a Poole-Frenkel mechanism involving defect states to free states has also been developed.

The simulated memristor structure is a metal-oxide-metal stack, with the metal regions each being 10nm thick and the oxide region being 30nm thick. The simulated cross-section is 250nm x 250nm, consistent with the experimental structures of [6]. The contact regions are assumed to be 10^{19} cm^{-3} n-doped silicon. The oxide material parameters are chosen to be those of Ta_2O_5. The simulated memristor is considered to be in series with a 50 ohm resistor, corresponding to the measuring scope input impedance and accounting for memristor capacitive displacement current.

Fig. 3 illustrates the model used for the calculations. This figure shows the conduction band-edge, the oxygen vacancy level and the electrochemical potential for the electrons as a function of position. This structure consists of a 30 nm TaO_x region between two electrodes. The energy barriers at the interfaces are assumed to be 1 eV in both cases. A bias of 0.1 V is used in agreement with the experiments.

The properties of the oxygen vacancies are not well known in these materials in spite of their importance in governing the transport. Thus the key properties were varied to obtain insight. For this figure, the vacancy concentration is set to be 10^{20} cm^{-3}. The energy of the 0/+ transition is assumed to be 0.3 eV for this figure. The energy of +/++ transition is assumed to be much larger, approximately 1 eV, and thus it is not considered in the calculations to be described.

Much band-bending occurs because the vacancies near the interfaces become ionized. The defect density is large enough that tunneling can take place from the electrodes into the oxide. Both free-to-free and free-to-defect tunneling were included in these calculations. However, only free-to-defect tunneling is included in the calculations used to produce Fig. 3.

The electrochemical potential is discontinuous at the interfaces. This fact and its constant value in the interior reveal that the transport is limited by the tunneling at the interfaces.

Fig. 4 shows the currents for two cases in which the vacancy concentration is varied. As expected, the factor of two increase in the vacancy concentration increases the current by a factor larger than two because tunneling has a non-linear dependence on this concentration.

An important effect of the barriers is an increase in the effect of the ionizing radiation. Thus the simple expression $I = qGV$ no longer applies. Thus much of the 10^7 discrepancy is removed.

The effect of hot electrons is also being explored. Each radiation injected electron has a temperature that is approximately given by the 3 eV bandgap of the oxide. This very large energy of the injected electrons tends to heat the electrons in the oxide region. Their density is small enough that this heating can be large. Furthermore, another effect is to increase the density of electrons in the higher energy regions in which the density was initially low. Thus it is expected that the current could be greatly increased.

The present results show that the heating has a large effect. This can be seen by an examination of the electron densities. However, the end result in these calculations is an initial reduction of the current for both cases. However, at long times, the current is increased in one case but decreased in the other case.

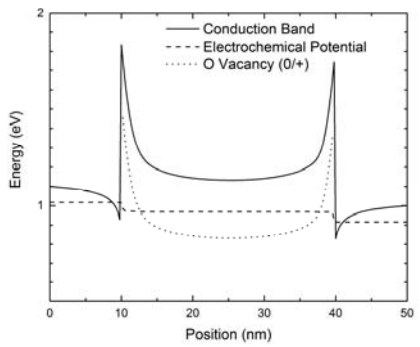

Figure 3: The conduction band-edge, electrochemical potential (ECP) and the oxygen vacancy state as discussed in the text. The discontinuity in the ECP reveals that tunneling limits the current.

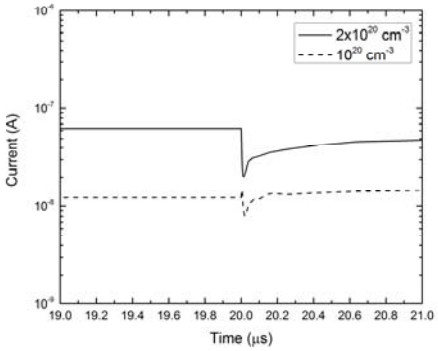

Figure 4: Dark currents and photocurrent for two values of oxygen vacancy concentrations as discussed in the text.

CONCLUSION

Our research has two primary implications. One is the development of a transport model for the dark current in the devices. This model takes into account tunneling at the interfaces. The other is an inclusion of heating effects caused by the ionizing radiation.

In further work, new information about the vacancy properties and concentrations will be used to refine the dark current model. Furthermore, a newly developed Poole-Frenkel tunneling mechanism will be applied to the transport problem. In addition, a more sophisticated model of the heating effects will be used to explore the effects of the ionizing radiation.

REFERENCES

[1] M.-J. Lee, C. B. Lee, D. Lee, S. R. Lee, M. Chang, J. H. Hur, Y.-B. Kim, C.-J. Kim, D. H. Seo, S. Seo, U. I. Chung, I.-K. Yoo and K. Kim, "A fast, high-endurance and scalable non-volatile memory device made from asymmetric Ta_2O_{5-x}/TaO_{2-x} bilayer structures," *Nat Mater,* vol. 10, no. 8, pp. 625-630, 2011.

[2] M. J. Marinella, S. M. Dalton, P. R. Mickel, P. E. Dodd, M. R. Shaneyfelt, E. Bielejec, G. Vizkelethy and P. G. Kotula, "Initial assessment of the effects of radiation on the electrical characteristics of TaO_x memristive memories," *IEEE Trans. Nucl. Sci.,* vol. 59, no. 6, pp. 2987-2994, 2012.

[3] D. R. Hughart, A. J. Lohn, P. R. Mickel, S. M. Dalton, P. E. Dodd, M. R. Shaneyfelt, A. I. Silva, E. Bielejec, G. Vizkelethy, M. T. Marshall, M. L. McLain and M. J. Marinella, "A comparison of the radiation response of TaO_x and TiO_2 memristors," *IEEE Trans. Nucl. Sci.,* vol. 60, no. 1, pp. 4512-4519, Dec. 2013.

[4] P. R. Mickel, A. J. Lohn, B. J. Choi, J. J. Yang, M.-X. Zhang, M. J. Marinella, C. D. James and R. S. Williams, "A physical model of switching dynamics in tantalum oxide memristive devices," *Applied Physics Letters,* vol. 102, no. 22, pp. 223502-5, 2013.

[5] R. Waser, R. Dittmann, G. Staikov and K. Szot, "Redox-Based Resistive Switching Memories – Nanoionic Mechanisms, Prospects, and Challenges," *Advanced Materials,* vol. 21, no. 25-26, pp. 2632-2663, 2009.

[6] M. L. McLain, H.P. Hjalmarson, T.J. Sheridan, P. R. Mickel, D. Hanson, K. McDonald, D.R. Hughart and M. J. Marinella, "The Susceptibility of TaO_x-Based Memristors to High Dose Rate Ionizing Radiation and Total Ionizing Dose," *IEEE Trans. Nucl. Sci.,* vol. 61, no. 6, pp. 2997-3004, Dec. 2014.

[7] M. Ieong, P.M. Solomon, S.E. Laux, H.-S.P. Wong and D. Chidambarrao, "Comparison of raised and Schottky Source/Drain MOSFETs Using a Novel Tunneling Contact Model," *IEDM,* 1998